Direct Experimental Determination of the Energy Barriers for Methyl Cation Transfer in the Reactions of Methanol with Protonated Methanol, Protonated Acetonitrile, and Protonated Acetaldehyde: A Low Pressure FTICR Study

Travis D. Fridgen,† Jonathan D. Keller, and Terry B. McMahon*,‡

Department of Chemistry, University of Waterloo, Waterloo, Ontario N2L 3G1, Canada

Received: November 29, 2000; In Final Form: January 23, 2001

Methyl cation transfer reactions between methanol and protonated methanol, protonated acetonitrile, and protonated acetaldehyde have been investigated experimentally by low-pressure FT-ICR mass spectrometry. The temperature dependencies of the rate constants for these reactions were determined in an Arrhenius-type analysis to obtain activation energies, enthalpies, and entropies of activation. The enthalpies of activation were determined to be -16.9 ± 0.6, -16.5 ± 0.6, and -18.4 ± 0.7 kJ mol^{-1} for the methanol/protonated methanol, methanol/protonated acetonitrile, and methanol/protonated acetaldehyde reactions, respectively. These values agree quite well with ab initio-calculated values. The entropies of activation were found to be quite similar for all three reactions within experimental uncertainty, which is expected due to the similar transition-state structures for all reactions. Ab initio potential energy surfaces calculated at the MP2/6-311G** level and basis set are reported for the three reactions. For the methanol/protonated acetonitrile and methanol/protonated acetaldehyde reactions, isomerization of the initially produced proton-bound dimer to a methyl-bound complex is suggested prior to methyl cation transfer. The barrier for the first isomerization is predicted to be significantly lower than the barrier for methyl cation transfer such that it does not interfere with the experimental determination of the latter.

Introduction

Alkyl cation transfer reactions are well-known reactions in the gas and condensed phases. For example, the Williamson synthesis of ethers occurs by transfer of an alkyl cation from an alkyl halide to an alkoxide anion through an S_N2 mechanism[1]

$$RO^- + R'-X \rightarrow ROR' + X^- \quad (1)$$

where R and R′ are alkyl groups and X is a halogen atom. Entirely analogous to these condensed phase reactions are the alkyl cation transfer reactions between protonated and neutral alcohols, in the gas phase, which eliminate water to produce protonated ethers[2−5]

$$ROH_2^+ + ROH \rightarrow R_2OH^+ + H_2O \quad (2)$$

These slow reactions are not limited to alcohols. Rate constants have been measured for alkyl cation transfer reactions between protonated alcohols, ethers, cyanides and thiols, and neutral alcohols, ethers, aldehydes, and cyanides[5−7] as well as others.[8−10] Thermochemical ladders corresponding to methyl cation affinities have also been constructed.[11,12]

One of the main goals of gas-phase ion chemistry is to obtain accurate kinetic and thermodynamic information which can be related to the potential energy surface, which governs reactivity. To this end, numerous experimental techniques have been devised;[13,14] some have specific applications, and others, such as Fourier transform ion cyclotron resonance mass spectrometry (FTICR-MS), are more broadly applicable. Thermodynamic properties of thousands of stable ionic species and gas-phase ion−molecule reactions have been determined.[15] Of equal importance to an accurate description of the potential energy surface, however, are the energetic positions corresponding to maxima or transition states, for which experimental values are scarce except for those determined by computational means.

Attempts have been made to determine the barriers to isomerization for ionic species. Refaey and Chupka[16] determined the barrier for isomerization of 1-propanol radical cation to its distonic isomer by observing the appearance energy for loss of water. Since loss of water from 1-propanol radical cation requires an intramolecular proton-transfer isomerization, which is the bottleneck for water loss,[17] the appearance energy for this reaction can be attributed to the isomerization barrier height. Booze and Baer used this energy barrier to obtain a RRKM model for the rate constant for water loss from 1-propanol radical cation measured by photoelectron photoion coincidence (PEPICO) experiments.[18] The value which they obtained for the heat of formation of the 1-propanol radical cation was in excellent agreement with an ab initio calculated value,[17] which was about 50 kJ mol^{-1} lower than the previous determination.

Mayer[19] has used a combination of metastable ion mass spectrometry, collision-induced dissociation mass spectrometry, and RRKM modeling with ab initio vibrational frequencies in an attempt to deduce the barrier height for isomerization of the proton-bound dimer of methanol and acetonitrile to an ion−molecule complex between $CH_3CNCH_3^+$ and H_2O

$$[CH_3OH - - H - - NCCH_3]^+ \rightarrow [CH_3CNCH_3 - - H_2O]^+ \quad (3)$$

† E-mail: tdfridge@sciborg.uwaterloo.ca.
‡ E-mail: mcmahon@sciborg.uwaterloo.ca.
* To whom all correspondence should be addressed.

10.1021/jp0043165 CCC: $20.00
Published on Web 03/24/2001

In these experiments, both N-methylated acetonitrile cation and protonated acetonitrile were observed,

$$[CH_3CNCH_3 - - H_2O]^+ \rightarrow CH_3CNCH_3^+ + H_2O \quad (4)$$

$$[CH_3OH - - H - - NCCH_3]^+ \rightarrow CH_3CNH^+ + CH_3OH \quad (5)$$

Since both of these products were observed, isomerization (eq 3) and the dissociation (eq 5) compete on the microsecond time scale. The transition-state energy for isomerization, then, is that required to give a rate constant comparable to the dissociation rate constant in the 10^5 s^{-1} regime. With this approach, the transition state was determined to lie 6 kJ mol^{-1} below the reactants at 298 K. More recently, a similar analysis on the reaction of protonated acetonitrile and ethanol (ethyl cation transfer) the isomerization barrier was determined to lie 22 kJ mol^{-1} lower than reactants.[20]

Recent work in our laboratory[7] has shown that, from an Arrhenius analysis of the temperature dependence of methyl cation exchange between protonated dimethyl ether and dimethyl ether forming trimethyloxonium cation and methanol, it is possible to obtain values for the energy barrier, as well as the change in enthalpy ($\Delta H^{\ddagger}$) and entropy ($\Delta S^{\ddagger}$) going from reactants to the transition state. These values, $\Delta H^{\ddagger} = -1.1 \pm 1.2$ kJ mol^{-1} and $\Delta S^{\ddagger} = -116 \pm 15$ J K^{-1} mol^{-1}, are in good agreement with the B3LYP/6-311G** calculated values of -4.6 kJ mol^{-1} and -132 J K^{-1} mol^{-1}, respectively.

In the present publication, we report the results of experiments on three methyl cation exchange reactions: (1) the reaction of protonated methanol with methanol producing protonated dimethyl ether and water, (2) the reaction of protonated acetonitrile with methanol to form N-methylated acetonitrile cation and water, and (3) the reaction of protonated acetaldehyde with methanol to form O-methylated acetaldehyde and water. An Arrhenius analysis of the temperature dependence of these three reactions is used to obtain purely experimental values of the activation energy barrier E_a, as well as $\Delta H^{\ddagger}$ and $\Delta S^{\ddagger}$, the differences in enthalpy and entropy, respectively, between reactants and the transition state for methyl cation exchange. These values are compared with those calculated by ab initio methods. In addition, calculated potential energy surfaces (PES) for the reactions of methanol with protonated acetonitrile and protonated acetaldehyde are presented and discussed.

Experimental Section

All experiments were carried out with a Bruker CMS 47 FT-ICR mass spectrometer equipped with a 4.7 T magnet. Vapor from samples of methanol (99.9%, BDH), acetonitrile (99.5%, Aldrich), and acetaldehyde (99.5%, Aldrich) were introduced into the ICR cell via a heated precision leak valves. The pressure inside the vacuum chamber was measured via a calibrated ionization gauge. The calibration of the ion gauge for the pressure of methanol was performed by measuring the rate of the following proton-exchange reaction

$$CH_3OH^{\bullet +} + CH_3OH \rightarrow CH_3OH_2^+ + CH_2OH^{\bullet} \quad (6)$$

for which the rate constant was assumed to be the collision rate constant, 2.3×10^{-9} cm^3 s^{-1} at 298 K. The calibration factor for the ion gauge was determined to be 2.25 ± 0.06 over the (calibrated) pressure range 9.8×10^{-9} to 1.0×10^{-7} mbar.

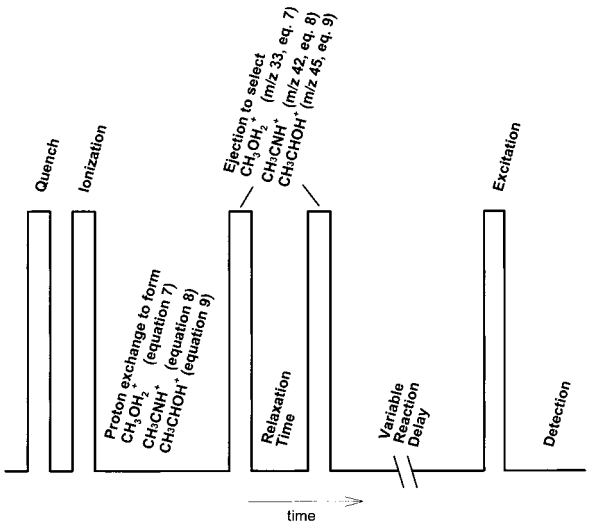

Figure 1. Scan function used for the FT-ICR experiments reported in this work.

The reactions studied here were the methyl cation transfer reactions given by eqs 7, 8, and 9.

$$CH_3OH_2^+ + CH_3OH \rightarrow (CH_3)_2OH^+ + H_2O \quad (7)$$

$$CH_3CNH^+ + CH_3OH \rightarrow CH_3CNCH_3^+ + H_2O \quad (8)$$

$$CH_3CHOH^+ + CH_3OH \rightarrow CH_3CHOCH_3^+ + H_2O \quad (9)$$

For each reaction, the pressure of neutral methanol was varied between calibrated pressures of 1.0×10^{-8} and 9.0×10^{-8} mbar. For reactions 8 and 9, the pressure in the ICR cell was increased by factors of between 1.5 and 2.5 with acetonitrile or acetaldehyde, respectively.

The pulse sequence used for these studies is shown in Figure 1. Ionization was done directly inside the ICR cell using 100 ms pulses of 70-eV electrons. The first delay after ionization is incorporated into the experiment in order to produce either $CH_3OH_2^+$ (*m*/*z* 33), CH_3CNH^+ (*m*/*z* 42), or CH_3CHOH^+ (*m*/*z* 45) by a series of proton-transfer reactions to the neutral precursor, after which all of the ions except the desired ionic precursor were ejected from the ICR cell by standard radio frequency (rf) ejection techniques. A second delay was incorporated in order to ensure thermal equilibrium of the ions, after which the ionic precursor of interest was once again isolated.

The temperature inside the ICR cell was measured in the following manner. An iron−constantan thermocouple was mounted on the outside of the ICR vacuum chamber and one was mounted inside the ICR cell. The temperature measured on the inside of the ICR cell was lower than that on the outside of the vacuum chamber. The temperature on the inside was calibrated to that on the outside. The temperatures reported here are those measured on the outside of the vacuum chamber but corrected to reflect the temperature inside the ICR cell.

The intensities of the precursor and product ions (including the ^{13}C contribution) were monitored typically until about 90% depletion of the precursor. The rate constants of methyl cation transfer for reactions 7−9 were obtained from a least-squares fitting of a semilogarithmic plot of normalized precursor ion intensity vs time. A typical mass spectrum for the reaction of protonated acetonitrile with methanol to form $CH_3CNCH_3^+$ and water is shown in Figure 2 after 10 and 80 s for the reaction conducted at 34 °C and a partial pressure of methanol of $3.7 \times$

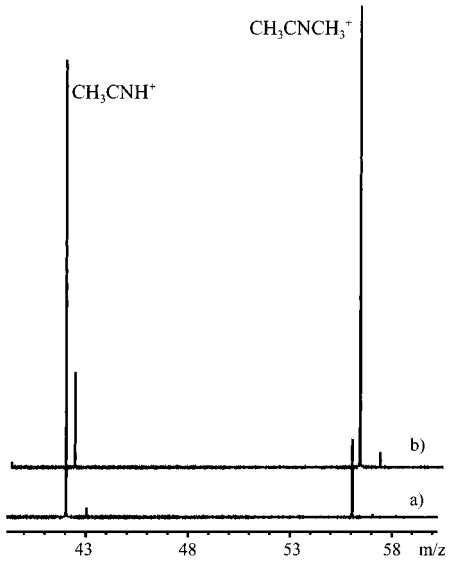

Figure 2. Mass spectra taken after delays of (a) 10 s and (b) 80 s of reaction between protonated acetonitrile with methanol to form $CH_3CNCH_3^+$ and water conducted at 34 °C and a partial pressure of methanol of 3.7×10^{-8} mbar. Note that spectrum b is shifted slightly to higher mass for clearity.

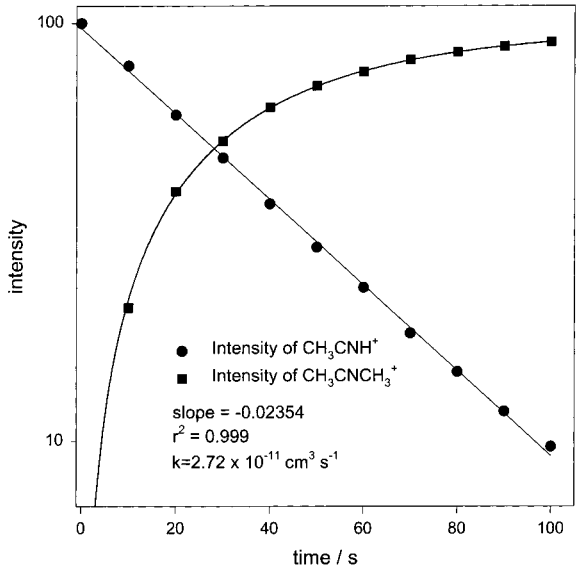

Figure 3. Semilogarithmic plot of intensity vs time for the reaction of protonated acetonitrile with methanol conducted at 34 °C and a partial pressure of methanol of 3.7×10^{-8} mbar.

10^{-8} mbar. The corresponding semilogarithmic plot of ion intensities vs time is shown in Figure 3.

Ab Initio Calculations. All calculations were performed at the MP2 level of theory in conjunction with the 6-311G** basis set utilizing Gaussian 98.[21] Transition-state structures were verified both by the presence of a single imaginary vibrational frequency corresponding to the vibrational mode in the correct reaction coordinate and by intrinsic reaction coordinate calculations.

Data Analysis and Arrhenius Theory. According to Arrhenius theory the rate constant of a chemical reaction varies with temperature according to the Arrhenius equation

$$\ln k = \ln A \frac{-E_a}{RT} \tag{10}$$

TABLE 1: Rate Constants for the Methyl Cation Exchange Reaction between Methanol and Protonated Methanol

temp/K	rate constant[a]
293	11.1 ± 0.1
296	10.4 ± 0.2
305	8.9 ± 0.3
311	8.1 ± 0.3
316	7.7 ± 0.3
323	6.9 ± 0.3
330	6.4 ± 0.1
334	6.2 ± 0.1
338	6.0 ± 0.3

[a] Rate constants in units of $10-11$ cm^3 molecule^{-1} s^{-1}.

where k is the rate constant, A is the preexponential or frequency factor, E_a is the activation energy, and R and T are the gas constant (8.314 kJ K^{-1} mol^{-1}) and Kelvin temperature, respectively. Thus from the slope, m, of a plot of ln k vs $1/T$, E_a and $\Delta H^{\ddagger}$, the activation energy and enthalpy of activation, respectively, can be obtained, according to eqs 11 and 12, respectively,

$$E_a = -mR \tag{11}$$

$$\Delta H^{\ddagger} = E_a - 2RT \tag{12}$$

From the thermodynamic formulation of transition state theory, the intercept of the Arrhenius plot A can be written in terms of the $\Delta S^{\ddagger}$,

$$A = \frac{k_b T}{h} e^2 e^{\Delta S^{\ddagger}/R} \tag{13}$$

where k_b is the Boltzmann constant. Thus from the intercept of the Arrhenius plot, $\Delta S^{\ddagger}$ can be determined. The errors in the rate constants represent only the standard deviation of the average rate constant, measured at various pressures, at each temperature. The slopes and intercepts as well as the error were calculated by using a least-squares regression where each point was weighted by the standard deviation in each point on the Arrhenius plot. These errors therefore reflect only random error. Systematic errors may be present. A nonuniform temperature within the ICR cell affects the absolute rate constant but has little effect on the temperature-dependent values reported here. For example, a five degree difference in temperature between the reported values and actual values would result in at most a 0.5 kJ mol^{-1} difference in E_a and a 1 J K^{-1} mol^{-1} difference in $\Delta S^{\ddagger}$.

Results and Discussion

$CH_3OH_2^+ + CH_3OH \rightarrow (CH_3)_2OH^+ + H_2O$. The methyl cation exchange reaction between methanol and protonated methanol was the only reaction observed in the ICR cell at all temperatures and pressures studied. This is contrary to other studies[22-24] which were complicated by a three-body association reaction forming the proton-bound dimer due to the higher pressures utilized.

$$CH_3OH_2^+ + CH_3OH + M \rightarrow (CH_3OH)_2H^+ M \tag{14}$$

One previous study by McMahon and Beauchamp[3] observed formation of the proton-bound dimer only when the pressures were above 10^{-4} Torr at reaction times on the order of 1 ms.

The rate constants for this reaction at the various temperatures studied showed no pressure dependence and are presented in Table 1. The rate constant at 296 K determined here was found

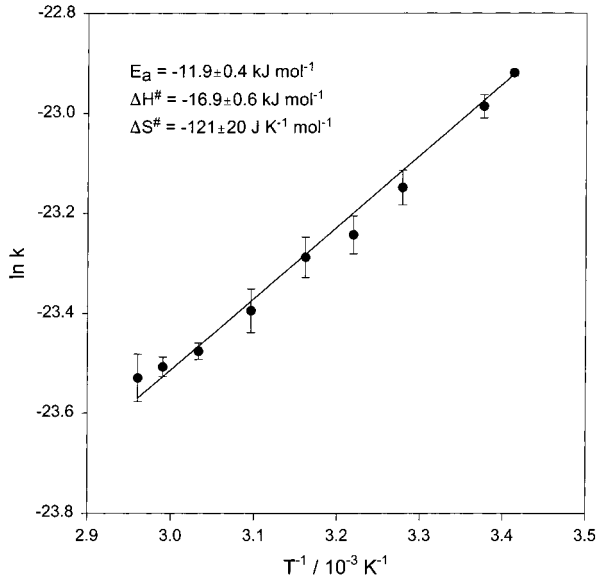

Figure 4. Arrhenius plot for the methyl cation transfer reaction of methanol with protonated methanol.

to be $(1.04 \pm 0.02) \times 10^{-10}$ cm^3 molecule^{-1} s^{-1} in excellent agreement with those obtained by McMahon and Beauchamp[3] of 1.0 and 1.1×10^{-10} cm^3 molecule^{-1} s^{-1}. In the latter case, the reaction was studied at pressures between 10^{-6} and 10^{-3} Torr. Bass et al.[23] obtained values between 0.7 and 1.2×10^{-10} cm^3 molecule^{-1} s^{-1} at a pressure of 5×10^{-4} Torr and at 300 K, where significant amounts of proton-bound dimer and trimer were also observed. Other values obtained for the rate constant for this reaction were approximately 0.8×10^{-10} cm^3 molecule^{-1} s^{-1} but were either complicated by significantly faster reactions[22] or were conducted at much higher pressures[24] where methyl cation transfer was the minor reaction observed. In those studies where temperature was varied,[23,24] a negative temperature dependence was observed, which agrees with our results in Table 1.

The Arrhenius plot for methyl cation transfer is shown in Figure 4. From the slope of this plot, values for E_a and $\Delta H^{\ddagger}$ of -11.9 ± 0.4 kJ mol^{-1} and -16.9 ± 0.6 kJ mol^{-1}, respectively, were obtained. Bouchoux and Choret[25] as well as Raghavachari et al.[26] calculated the enthalpy of activation to be -26 (MP2/6-31G*) and -21 kJ mol^{-1} (HF/6-31G**), respectively. Both of these values are slightly lower than our experimental values. We have also calculated a potential energy surface for this reaction at the MP2 level with a more extensive basis set (6-311G**) than that used by Bouchoux and Choret.[25] The potential energy surface and structures are shown Figures 5 and 6, respectively. The barrier height for methyl cation transfer, based on these calculations, is found to be -15.8 kJ mol^{-1}, which is in excellent agreement with the experimentally determined value.

From the intercept of the Arrhenius plot a value for $\Delta S^{\ddagger}$ of -121 ± 20 J K^{-1} mol^{-1}. This value is quite similar to the entropy differences determined for clustering of protonated methanol and methanol, which has been determined to be about -120 J K^{-1} mol^{-1}.[27] For a tight transition state such as that suggested, shown in Figures 5 and 6, the entropy of activation would be expected to be slightly more negative than that determined here experimentally, but certainly within the reported uncertainty.

$CH_3CNH^+ + CH_3OH \rightarrow CH_3CNCH_3^+ + H_2O$. The rate of the reaction between protonated acetonitrile and methanol was found to not be dependent upon the pressure of acetonitrile in the ICR cell. For example, for the reaction at 296 K, and a calibrated methanol pressure of 5.2×10^{-9} mbar, the rate constants were determined to be 5.44×10^{-11} and 5.66×10^{-11} cm^3 s^{-1} at (uncalibrated) acetonitrile pressures of 5.8×10^{-9} and 1.2×10^{-8} mbar, respectively. Furthermore, the only reaction observed at all temperatures and pressures was the methyl cation exchange reaction.

The rate constants obtained for the methyl cation exchange between methanol and protonated acetonitrile are listed in Table 2. The Arrhenius plot for this reaction is given in Figure 7. The slope of this plot yields a value for the activation energy

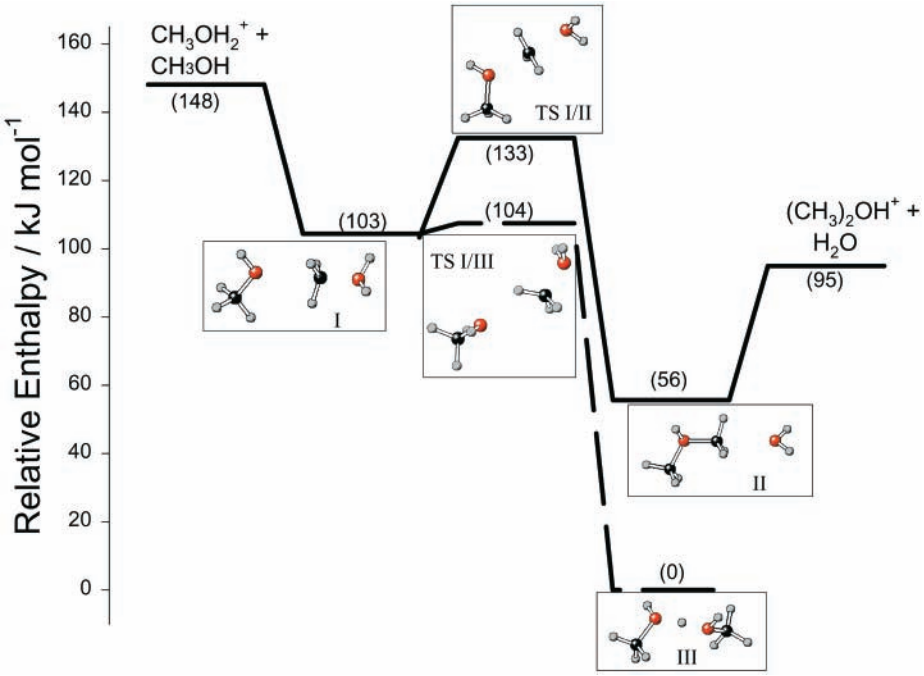

Figure 5. MP2/6-311G** calculated potential-energy surface for the methanol/protonated methanol reaction. Geometries for stationary points are shown in Figure 6.

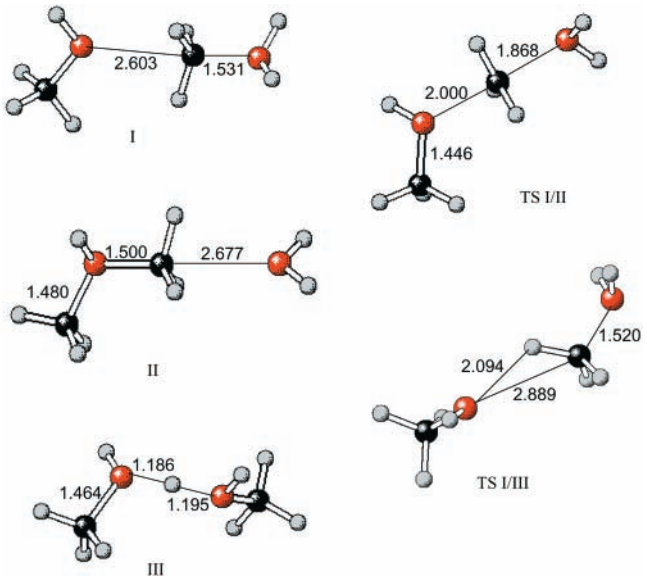

Figure 6. MP2/6-311G** calculated structures for the stationary points on the methanol/protonated methanol potential-energy surface of Figure 5.

TABLE 2: Rate Constants for the Methyl Cation Exchange Reaction between Methanol and Protonated Acetonitrile

temp/K	rate constant[a]
293	3.49 ± 0.08
296	3.4 ± 0.1
307	2.8 ± 0.2
313	2.5 ± 0.2
320	2.4 ± 0.1
331	2.07 ± 0.08
335	1.89 ± 0.07

[a] Rate constants in units of 10^{-11} cm^3 molecule^{-1} s^{-1}.

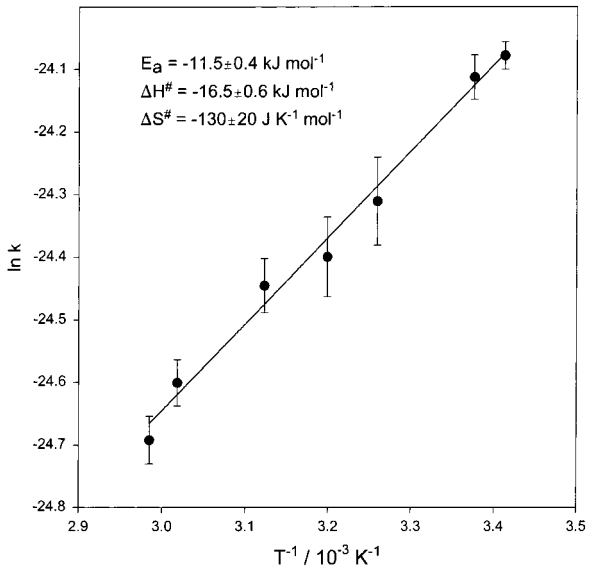

Figure 7. Arrhenius plot for the methyl cation transfer reaction of methanol with protonated acetonitrile.

of -11.5 ± 0.4 kJ mol^{-1} and an enthalpy of activation of -16.5 ± 0.6 kJ mol^{-1}. The enthalpy of activation, at 298 K, obtained by Mayer[19] was -6 kJ mol^{-1}, which corresponds to a 10 kJ mol^{-1} higher enthalpy of activation compared to our experimentally determined value. It should be noted, however, that the value determined by Mayer is a prediction based on a number of assumptions. First of all, in the RRKM modeling, experimental unimolecular rate constants were assumed to be approximately 10^5 s^{-1}, based on the residence time of the ions within the flight path of the mass spectrometer. Since methyl cation transfer and simple bond cleavage (producing reactants) are in competition, based on the MI spectra, a value for $\Delta H^{\ddagger}$ which caused the log k vs internal energy of the proton-bound dimer to cross in the region where the rate constants were $\sim 10^5$ s^{-1}, was assigned. This analysis has an element of subjectiveness to it. Furthermore, the use of ab initio vibrational frequencies for the proton-bound dimer and vibrational frequencies for the transition states fitted to produce characteristic entropy differences between the proton bound dimer and transition states adds another element of uncertainty. In contrast, the enthalpy of activation determined here is purely experimental. Our determinations of the experimental enthalpies of activation for the $CH_3OH_2^+ + CH_3OH$ methyl cation transfer (above) and that determined previously for the $(CH_3)_2OH^+ + (CH_3)_2O$ methyl cation transfer[7] are in excellent agreement with ab initio calculations. This lends confidence that our $\Delta H^{\ddagger} = -16.5 \pm 0.6$ kJ mol^{-1} is a dependable value. The value predicted by Mayer, however, is not unreasonable given the approximate method of its estimation.

Mayer also presented a calculated potential energy surface (PES) for this reaction,[19] however, the potential energy profile for the rearrangement of the proton-bound dimer of methanol and acetonitrile to the methylated acetonitrile cation/water complex was assumed to be a direct isomerization. The barrier for this isomerization was calculated to be approximately 110 kJ mol^{-1}, considerably in excess of the barrier estimated by Mayer and by our experimental value. Mayer did conclude that there must be an alternative route for this isomerization. Our calculated PES for this reaction is shown in Figure 8. It includes an isomerization of the proton-bound dimer to a structure which has the nitrogen of acetonitrile electrostatically bound to the methyl group of protonated methanol. The structures are given in Figure 9. An analogous structure was predicted to precede methyl cation transfer for both the methanol/protonated methanol[25,26] and dimethyl ether/protonated dimethyl ether[7] reactions. This type of structure was first suggested by Kleingeld and Nibbering.[4] It is important to note, however, that the transition state for isomerization of the proton-bound dimer to the electrostatically bound complex is not the bottleneck for methyl cation exchange, since it is calculated to be 25 kJ mol^{-1} lower in energy than the transition state for actual methyl cation transfer. The calculated $\Delta H^{\ddagger}$ is -21.5 kJ mol^{-1}, in fairly good agreement with our experimentally determined value of -16.5 ± 0.6 kJ mol^{-1}.

It should be noted that the relative energies of the proton-bound dimer and the two minima on the right-hand side of the methyl cation exchange barrier agree fairly well with the calculations of Mayer.

From the intercept of the Arrhenius plot in Figure 7 and eq 13, an entropy of activation value of -130 ± 20 J K^{-1} mol^{-1} was obtained, which is consistent with what is expected for a tight transition state. This experimental value is in good agreement with the calculated value of -111 J K^{-1} mol^{-1}.

$CH_3CHOH^+ + CH_3OH \rightarrow CH_3CHOCH_3^+ + H_2O$. The chemistry occurring in the acetaldehyde/methanol mixtures was slightly more complicated. At the lowest temperatures used, two very minor side reactions, one producing m/z 43 and one producing m/z 47, in addition to the dominant methyl cation transfer forming O-methylated acetaldehyde, were observed.[28] The m/z 43 ion predominates over the m/z 47 ion at high acetaldehyde pressure and is produced by hydride abstraction

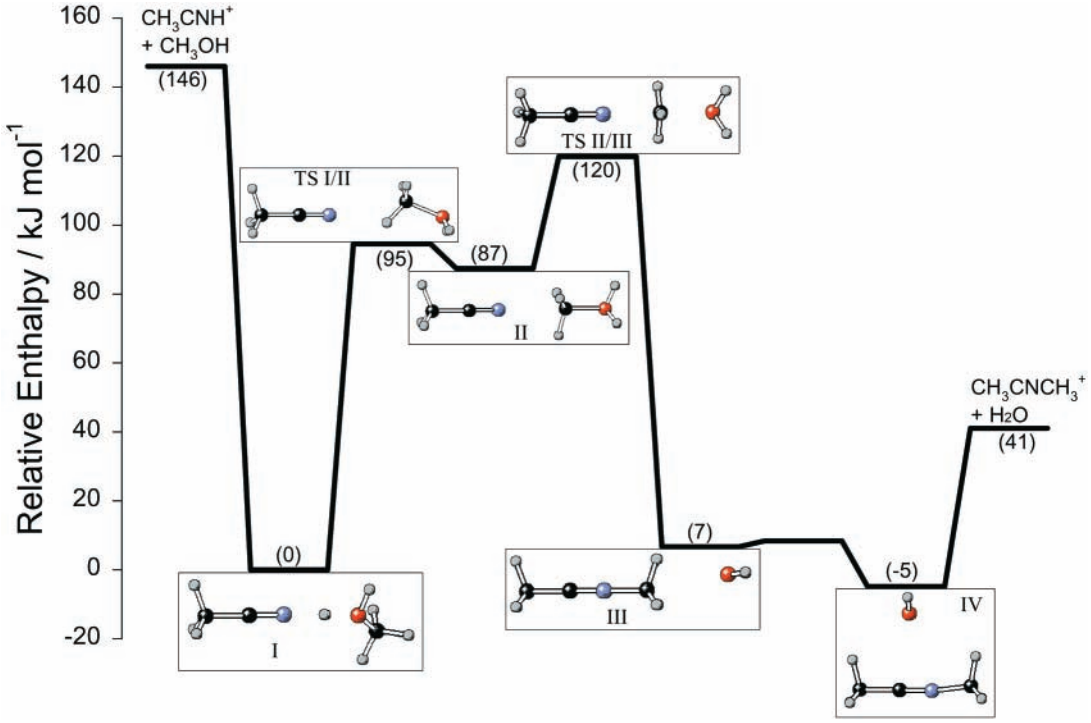

Figure 8. MP2/6-311G** potential-energy surface for the reaction of methanol with protonated acetonitrile. Geometries for stationary points are shown in Figure 9.

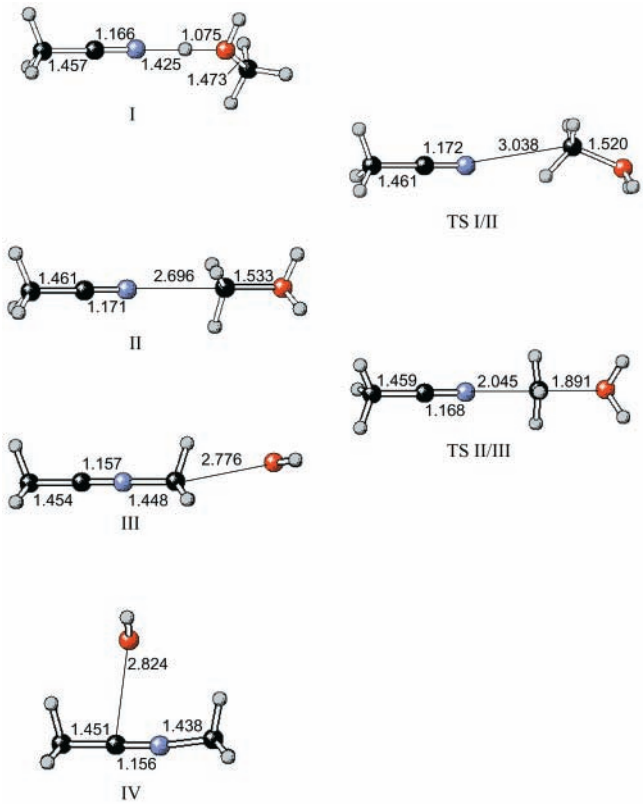

Figure 9. MP2/6-311G** calculated structures for the stationary points on the methanol/protonated acetonitrile potential-energy surface in Figure 8.

from neutral acetaldehyde by protonated acetaldehyde forming CH_3CO^+ and neutral ethanol,[29]

$$CH_3CHOH^+ + CH_3CHO \rightarrow CH_3CO^+ + CH_3CH_2OH \quad (15)$$

At higher methanol pressures the occurrence of *m*/*z* 47 predominates over *m*/*z* 43 and, so, is very likely to be produced from a reaction with methanol. König et al.[30] also observed *m*/*z* 47 in their reactions of protonated acetaldehyde and methanol and assigned it to protonated dimethyl ether formed following proton transfer from protonated acetaldehyde to methanol followed by a methyl cation transfer reaction with methanol. The assignment of this mechanism was confirmed by deuterium isotope labeling experiments. This mechanism involves a proton transfer which is endothermic by some 14 kJ mol^{-1} and thus is expected to be quite slow if it were to occur in the ICR cell and the rate would increase with methanol pressure as was observed. A methyl cation transfer reaction from protonated acetaldehyde to methanol (eq 16) is less likely, since it is endothermic by 320 kJ mol^{-1}. Even if the neutral loss was assumed to be formaldehyde, which would require a concerted mechanism, this would be endothermic by 41 kJ mol^{-1}.

$$CH_3CHOH^+ + CH_3OH \rightarrow (CH_3)_2OH^+ + :CHOH \quad (16)$$

The proton-transfer reaction forming protonated methanol and subsequent methylation to form *m*/*z* 47 was not observed in the acetonitrile system, since proton transfer from protonated acetonitrile to methanol is endothermic by 25 kJ $mol{-}^{1}$.

The two side reactions forming *m*/*z* 43 and 47 become even less important at higher temperatures and these ions were too weak in intensity to obtain meaningful kinetics. It is important to note that in experiments conducted where no methanol was present, absolutely no *m*/*z* 59 ($CH_3CHOCH_3^+$) was produced, which rules out the possibility of methyl cation transfer between acetaldehyde and protonated acetaldehyde. The temperature-dependent rate constants are tabulated in Table 3 and it is apparent that the rate constant for the reaction of protonated acetaldehyde with methanol (methyl cation transfer) decreases with temperature as expected.

The Arrhenius plot for the methyl cation exchange reaction between methanol and protonated acetaldehyde is presented in Figure 10. From the slope of the Arrhenius plot values for E_a

TABLE 3: Rate Constants for the Methyl Cation Exchange Reaction between Methanol and Protonated Acetaldehyde

temp/K	rate constant[a]
294	12.7 ± 0.4
297	12.1 ± 0.2
304	10.4 ± 0.4
310	9.3 ± 0.4
314	8.9 ± 0.6
322	7.7 ± 0.3
327	7.4 ± 0.2
335	6.6 ± 0.1

[a] Rate constants in units of 10^{-12} cm^3 molecule^{-1} s^{-1}.

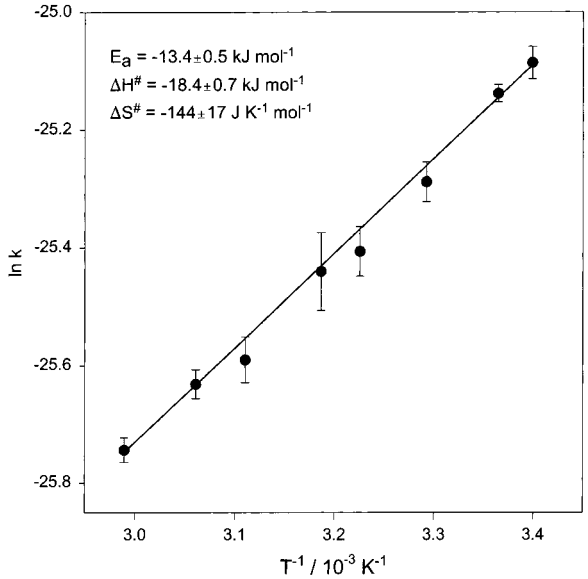

Figure 10. Arrhenius plot for the methyl cation transfer reaction of methanol with protonated acetaldehyde.

and $\Delta H^{\ddagger}$ of -13.4 ± 0.5 and -18.4 ± 0.7 kJ mol^{-1}, respectively, were obtained. The value for $\Delta H^{\ddagger}$ is in good agreement with the calculated value of -16.7 kJ mol^{-1}.

The calculated PES is given in Figure 11 and the structures are given in Figure 12. As in the preceding cases, the originally formed proton-bound dimer must isomerize to an isomer, which has the methyl group of protonated methanol electrostatically bound to the oxygen of acetaldehyde. The barrier to this first isomerization is, once again, not the bottleneck for this reaction as it is lower in energy than the transition state for methyl cation transfer by 30 kJ mol^{-1}.

From the intercept of the plot in Figure 10, an entropy of activation of -144 ± 17 J K^{-1} mol^{-1} was obtained and is in acceptable agreement with the calculated value of -128 J K^{-1} mol^{-1}.

Comparison of Methyl Cation Transfer Reactions. In Table 4 the thermodynamic parameters pertaining to the transition states for each of the methyl cation transfer reactions studied to date by low-pressure FT-ICR mass spectrometry are summarized. The first three methyl cation transfer reactions summarized in Table 4 are different from the protonated dimethyl ether/dimethyl ether reaction in that water is eliminated in the former three and methanol is eliminated in the latter case. It is interesting to note how close the experimental enthalpies of activation are to each other for the cases of methyl cation transfer between methanol and either protonated methanol, protonated acetonitrile, or protonated acetaldehyde. In fact, within the reported uncertainty there is virtually no difference in the enthalpies of activation observed except for a slightly lower barrier in the case of protonated acetaldehyde. In the case of methyl cation transfer between protonated dimethyl ether and dimethyl ether,[7] the enthalpy of activation is significantly higher, ca. 15 kJ mol^{-1}. Some insight into this comes from comparing the calculated activation energies on going from the complex just preceding methyl cation transfer, where the methyl group of protonated methanol is electrostatically bound to the methyl cation acceptor site, to the transition states for methyl cation transfer for all reactions. These calculated energy differences are strikingly close, 29, 33, 31, and 30 kJ mol^{-1} for the protonated methanol/methanol, protonated acetonitrile/methanol, protonated acetaldehyde/methanol, and protonated dimethyl ether/dimethyl ether[7] reactions, respectively. The electrostatically bound complex preceding methyl cation transfer is much less energetically favored for the protonated dimethyl ether/dimethyl ether system, compared to separated reactants, than for each of the other systems. The calculations show that the barriers for methyl cation transfer from the methyl-bound complex are virtually the same.

An interesting feature of the potential energy surfaces reported here for methanol/protonated acetonitrile and methanol/protonated acetaldehyde is that methyl cation transfer is preceded by an isomerization of the proton-bound dimer to structures where methanol is protonated and its methyl group is electrostatically bound to the nitrogen or oxygen of acetonitrile or acetaldehyde, respectively. In a recent report it was shown that for the reaction of dimethyl ether and protonated dimethyl ether the structure in the entrance channel is the complex with a methyl group of protonated dimethyl ether electrostatically bound to the oxygen of dimethyl ether.[31] This was rationalized by a combination of ab initio calculations and the strong temperature dependence of the dissociation rate constant of the nascent proton-bound dimer. The high-energy complex, then, either rearranges to form the proton-bound dimer or undergoes methyl cation exchange to form trimethyloxonium cation and methanol. In the case of methanol/protonated methanol one reported potential energy surface has the proton-bound dimer in the entrance channel followed by rearrangement to the methyl-bound structure and then methyl cation transfer.[25] This perspective contradicts experiments which have been reported using ^{18}O-labeled protonated methanol.[32−34]

$$CH_3{}^{18}OH_2{}^+ + CH_3{}^{16}OH \rightarrow (CH_3)_2{}^{18}OH^+ + H_2{}^{16}O \quad (17a)$$

$$CH_3{}^{18}OH_2{}^+ + CH_3{}^{16}OH \rightarrow (CH_3)_2{}^{16}OH^+ + H_2{}^{18}O \quad (17b)$$

If the reaction in eq 17 produces a 50/50 mixture of labeled to unlabeled protonated dimethyl ether, then the proton-bound dimer is the species in the entrance channel for this reaction. However, Graul and Squires[32] obtained a ratio of 2/1 for 17b/17a and Dang and Bierbaum[33] as well as McMahon[34] obtained a value of 1.2/1. The fact that reaction 17b appears to be favored would indicate that a certain portion of the reactions producing protonated dimethyl ether go via a direct S_N2 mechanism and thus the methyl-bound complex should be in the entrance channel for reaction of protonated methanol and methanol. Since isomerization of this complex to the proton-bound dimer has a lower energy requirement than methyl cation transfer, the proton-bound dimer/methyl-bound complex isomerization reactions are fairly rapid, which is why the reaction in eq 17 does not solely produce $(CH_3)_2{}^{16}OH^+$. It is proposed then that, like the protonated dimethyl ether/dimethyl ether PES, formation of a methyl-bound complex precedes proton-bound dimer formation and methyl cation transfer and this is depicted in

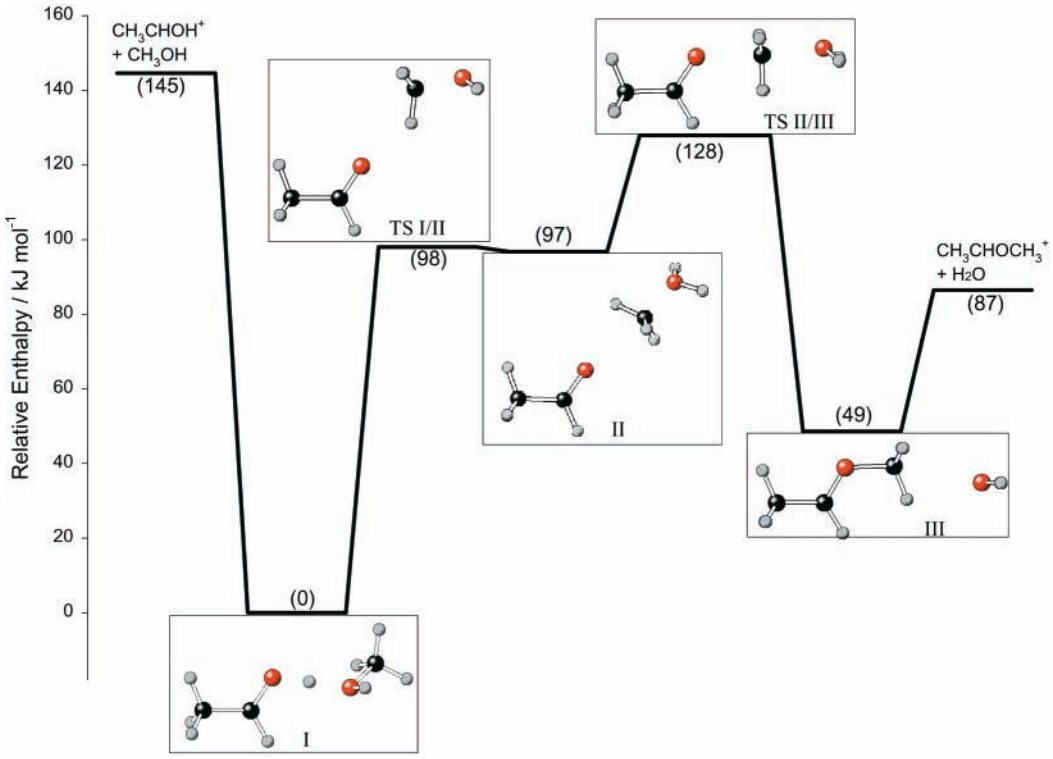

Figure 11. MP2/6-311G** potential-energy surface for the reaction of methanol with protonated acetaldehyde. Geometries for stationary points are shown in Figure 12.

TABLE 4: Summary of Thermodynamic Parameters Pertaining to the Transition State for Methyl Cation Transfer Obtained from Low-Pressure FT-ICR Experiments

	$CH_3OH_2^+ + CH_3OH$		$CH_3CNH^+ + CH_3OH$		$CH_3CHOH^+ + CH_3OH$		$(CH_3)_2OH^+ + (CH_3)_2OH$[c]	
	exptl	calcd	exptl	calcd	exptl	calcd	exptl	calcd
$\Delta H^{\ddagger}$[a]	-16.9 ± 0.6	-15.8	-16.5 ± 0.6	-21.5	-18.4 ± 0.7	-16.7	-1.07 ± 0.33	-4.6
$\Delta S^{\ddagger}$[b]	-121 ± 20	-150	-130 ± 20	-111	-144 ± 17	-128	-116 ± 15	-132
$\Delta G^{\ddagger}$[a](298)	19 ± 6	28.9	22 ± 6	11.2	25 ± 5	18.5	34 ± 5	34.8

[a] kJ mol^{-1}. [b] J K^{-1} mol^{-1}. [c] Products are trimethyloxonium cation and methanol from ref 7.

Figure 5. Further support of the methyl-bound complex being in the entrance channel for reaction between protonated methanol and methanol comes from calculations where the O−H bond of the proton-bound dimer was stretched and frozen and geometry optimizations were performed. This resulted in an expected increase in energy, but also, the structure collapsed to the methyl-bound complex structure.

The entropies of activation for all four reactions are, within the reported uncertainties very much the same, which is expected given the similarities of the transition structures associated with each of the reactions. Since the experimental and calculated barrier heights are all very close in energy, entropy must be the reason for the slower rates of reaction for the protonated acetonitrile and protonated acetaldehyde reactions. In fact, the experimentally determined $\Delta S^{\ddagger}$ values are seen to decrease over the series, protonated methanol/methanol (-121 ± 20 J K^{-1} mol^{-1}), protonated acetonitrile/methanol (-130 ± 20 J K^{-1} mol^{-1}), protonated acetaldehyde/methanol (-144 ± 17 J K^{-1} mol^{-1}). Therefore, the transition states become tighter over this series.

Structures of the Proton-Bound Dimers. An interesting feature pertaining to the structure of the methanol/acetonitrile proton-bound dimer (see Figure 9) is that the O−H bond length is 1.075 Å, while the N−H bond length is 1.425 Å, and the proton affinity of methanol is significantly lower than that of acetonitrile (ΔPA = 24.9 kJ mol-1).[15] Mayer's proton-bound dimer structure for methanol/acetonitrile (MP2/6-31+G*) set the bond lengths very close to those reported here at 1.075 and 1.475 Å for the O−H and N−H bond lengths, respectively.[19] Based on the proton affinities of the monomers alone, it might have been expected that the proton should be closer to the monomer of higher proton affinity. However, the dipole moment of acetonitrile is 3.92 D, while the dipole moment of methanol is substantially smaller at 1.70 D. At the minimum-energy structure of the proton-bound dimer, the calculated dipole moment of the dimer is 1.60 D. By stretching and freezing the O−H bond at 1.5 Å, the N−H bond length shortens to 1.094 Å, while the energy of the system rises 22 kJ mol^{-1} and the dipole moment rises to 3.41 D. MP2/6-31+G* calculations by Ochran et al.[20] on the proton-bound dimer of ethanol and acetonitrile show the O−H and N−H bond lengths to be 1.060 and 1.519 Å, respectively, even though acetonitrile has a slightly higher proton affinity.[15] The difference in dipole moments is very similar for these two species. It seems as though increasing the magnitude of the ion−dipole interaction in the dimer and thus lowering the overall dipole moment of the dimer, by associating the proton with the lower dipole moment species, is a factor in lowering the energy of the proton-bound dimer.

The structure of the proton-bound dimer of acetaldehyde and methanol in Figure 12 shows that the acetaldehyde O−H bond is 1.167 Å, while the methanol O−H bond is *slightly larger* at 1.226 Å. The proton affinity of acetaldehyde is 10.7 kJ mol^{-1}, larger than that of methanol,[15] and the dipole moments are 2.69 and 1.70 D, respectively. Both the difference in dipole moments and proton affinities between acetaldehyde and methanol are

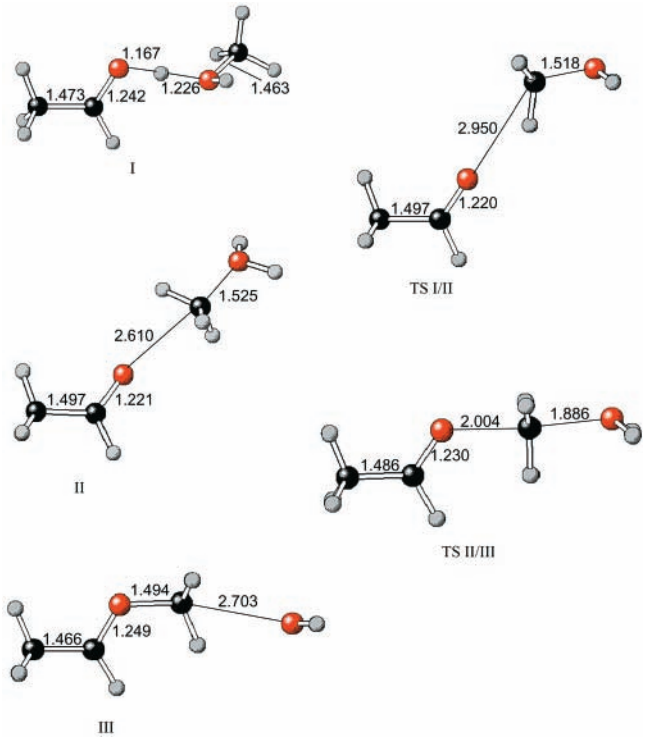

Figure 12. MP2/6-311G** calculated structures for the stationary points on the methanol/protonated acetaldehyde potential-energy surface in Figure 11.

less than those between acetonitrile and methanol. The resulting proton-bound methanol/acetaldehyde dimer therefore does not show quite the same structural peculiarity as the methanol/acetonitrile proton-bound dimer. The dipole moment of the proton-bound dimer is 1.74 D. On the basis of the proton affinities alone, however, one would expect the difference in the acetaldehyde O−H and methanol O−H bond to be greater than predicted by the calculations. Clearly, further study is necessary to demonstrate an overall trend.

Conclusions

The enthalpies and entropies of activation as well as the activation energies for the methyl cation transfer reactions between methanol and protonated methanol and between protonated acetonitrile and protonated acetaldehyde have been determined experimentally by low-pressure FT-ICR mass spectrometry. The enthalpies and entropies for these reactions are, within experimental uncertainty, quite similar, which is expected since the transition-state structures are all quite similar. The methyl cation transfer reaction is preceded by isomerization of the proton-bound dimer to a methyl-bound complex for the reactions of methanol with protonated acetonitrile and protonated acetaldehyde. It is proposed that for the reaction of methanol with protonated methanol, the methyl-bound complex is in the entrance channel. This methyl-bound complex then either isomerizes to the proton-bound dimer (reversible) or undergoes methyl cation transfer.

The experimental entropies of activation suggest that the transition state for methyl cation transfer increase in tightness over the series of reactions going from protonated methanol to protonated acetonitrile to protonated acetaldehyde.

Acknowledgment. The financial support of the Research Grants Program of the Natural Sciences and Engineering Research Council of Canada (NSERC) is acknowleged. T.D.F. gratefully acknowledges the Posdoctoral Fellowship granted by NSERC. We acknowledge the thorough reading and helpful comments by the referees.

References and Notes

(1) *Organic Chemistry*, 6th ed.; Morrison, R. T., Boyd, R. N., Eds.; Prentice Hall: Englewood Cliffs, NJ, 1992.
(2) Hall, D. G.; Gupta, C.; Morton, T. H. *J. Am. Chem. Soc.* **1981**, *103*, 2416.
(3) McMahon, T. B.; Beauchamp, J. L. *J. Phys. Chem.* **1977**, *81*, 593.
(4) Kleingeld, J. C.; Nibbering, N. M. M. *Org. Mass Spectrom.* **1982**, *17*, 136.
(5) Karpas, Z.; Meot-Ner, M. *J. Phys. Chem.* **1989**, *93*, 1859.
(6) Meot-Ner, M.; Karpas, Z. *J. Phys. Chem.* **1986**, *90*, 2206.
(7) Fridgen, T. D.; McMahon, T. B. *J. Am. Chem. Soc.*, in press.
(8) Herman, J. A.; Xu, G.; Herman, K.; McMahon, T. B. *Int. J. Mass Spectrom. Ion Processes* **1992**, *113*, 143.
(9) Szulejko, J. E.; Fisher, J. J.; McMahon, T. B.; Wronka, J. *Int. J. Mass Spectrom. Ion Processes* **1988**, *83*, 147.
(10) Wilson, P. F.; McEwan, M. J.; Meot-Ner, M. *Int. J. Mass Spectrom. Ion Processes* **1994**, *132*, 149.
(11) McMahon, T. B.; Heinis, T.; Nicol, G.; Hovey, J. K.; Kebarle, P. *J. Am. Chem. Soc.* **1988**, *110*, 7591.
(12) Deakyne, C. A.; Meot-Ner, M. *J. Phys. Chem.* **1990**, *94*, 232.
(13) Concise descriptions and application of the various methods have been consolidated in: (a) *Techniques for the Study of Ion−Molecule Reactions;* Farrar, J. M., Saunders, W. H., Jr., Eds.; John Wiley & Sons: Toronto, 1988. And (b) *Advances in Gas-Phase Ion Chemistry*; Adams, N. G., Babcock, L. M., Eds.; JAI Press Inc.: Greenwich, CT, 1996.
(14) As well, there are four review articles by the following sets of authors: (a) Bowers, M. T.; Kemper, P. R.; van Koppen, P.; Wyttenbach, T.; Carpenter, C. J.; Weis, P.; Gidden, J.; (b) McMahon, T. B.; (c) Luis, J.; Abboud, M.; Notario, R.; (d) Baer, T.; Lafleur, R.; Mazyar, O. In *Energetics of Stable Molecules and Reactive Intermediates*; Minas da Piedade, M. E., Ed.; Kluwer Academic Press: Boston, 1999.
(15) NIST Chemistry WebBook, NIST Standard Reference Database Number 69; Mallard, W. G., Linstrom, P. J., Eds.; National Institute of Standards and Technology: Gaithersburg, MD, February 2000; 20899 (http://webbook.nist.gov).
(16) Refaey, K. M. A.; Chupka, W. A. *J. Chem. Phys.* **1968**, *48*, 5205.
(17) Booze, J. A.; Baer, T. *J. Phys. Chem.* **1992**, *96*, 5710.
(18) Booze, J. A.; Baer, T. *J. Phys. Chem.* **1992**, *96*, 5715.
(19) Mayer, P. M. *J. Phys. Chem. A* **1999**, *103*, 3687.
(20) Ochran, R. A.; Annamalai, A.; Mayer, P. M. *J. Phys. Chem. A* **2000**, *104*, 8505.
(21) Gaussian 98, Revision A.7; Frisch, M. J., Trucks, G. W., Schlegel, H. B., Scuseria, G. E., Robb, M. A., Cheeseman, J. R., Zakrzewski, V. G., Montgomery, J. A., Jr., Stratmann, R. E., Burant, J. C., Dapprich, S., Millam, J. M., Daniels, A. D., Kudin, K. N., Strain, M. C., Farkas, O., Tomasi, J., Barone, V., Cossi, M., Cammi, R., Mennucci, B., Pomelli, C., Adamo, C., Clifford, S., Ochterski, J., Petersson, G. A., Ayala, P. Y., Cui, Q., Morokuma, K., Malick, D. K., Rabuck, A. D., Raghavachari, K., Foresman, J. B., Cioslowski, J., Ortiz, J. V., Baboul, A. G., Stefanov, B. B., Liu, G., Liashenko, A., Piskorz, P., Komaromi, I., Gomperts, R., Martin, R. L., Fox, D. J., Keith, T., Al-Laham, M. A., Peng, C. Y., Nanayakkara, A., Gonzalez, C., Challacombe, M., Gill, P. M. W., Johnson, B., Chen, W., Wong, M. W., Andres, J. L., Gonzalez, C., Head-Gordon, M., Replogle, E. S., Pople, J. A., Eds.; Gaussian, Inc.: Pittsburgh, PA, 1998.
(22) Vogt, J.; Beauchamp, J. L. *J. Am. Chem. Soc.* **1975**, *97*, 6682.
(23) Bass, L. M.; Cates, R. D.; Jarrold, M. F.; Kirchner, N. J.; Bowers, M. T. *J. Am. Chem. Soc.* **1983**, *105*, 7024.
(24) Morris, R. A.; Viggiano, A. A.; Paulson, J. F.; Henchman, M. J. *J. Am. Chem. Soc.* **1991**, *113*, 5932.
(25) Bouchoux, G.; Choret, N. *Rapid Commun. Mass Spectrom.* **1997**, *11*, 1799.
(26) Raghavachari, K.; Chandrasekhar, J.; Burnier, R. C. *J. Am. Chem. Soc.* **1984**, *106*, 3124.
(27) (a) Meot-Ner, M. *J. Am. Chem. Soc.* **1992**, *114*, 3312. (b) Larson, J. W.; McMahon, T. B. *J. Am. Chem. Soc.* **1982**, *104*, 6255.
(28) Dolnikowski, G. G.; Heath, T. G.; Watson, J. T.; Scrivens, J. H.; Rolando, C. H. *J. Am. Chem. Soc. Mass Spectrom.* **1990**, *1*, 481.
(29) Tzeng, W. B.; Wei, S.; Castleman, A. W., Jr. *Chem. Phys. Lett.* **1990**, *168*, 30.
(30) König, S.; Kofel, P.; Reinhard, H.; Sägesser, M.; Schlunegger, U. P. *Org. Mass Spectrom.* **1993**, *28*, 1101.
(31) Fridgen, T. D.; McMahon, T. B. *J. Phys. Chem. A* **2001**, *105*, 1011.
(32) Graul, S. T.; Squires, R. R. *Int. J. Mass Spectrom. Ion Processes* **1987**, *81*, 183.
(33) Dang, T. T.; Bierbaum, V. M. *Int. J. Mass Specrom. Ion Processes* **1992**, *117*, 65.
(34) McMahon, T. B., unpublished results.